

Synthesis, Fluorescence, and Antifungal Activity of a Bifunctional Lead (II) Coordination Polymer Based on Multidentate Acylhydrazone Ligand

Chengfang Qiao,[†] Xia Gao,[†] Qi Tang,[†] Jianfang Wang,[†] Yulin Gao,[†] Meili Zhang,[†] Zhengqiang Xia^{‡,*}, Haitao Han,[‡] Chunxin Zhao,[‡] and Chunsheng Zhou^{†,*}

[†]Shaanxi Key Laboratory of Comprehensive Utilization of Tailings Resources, College of Chemical Engineering and Modern Materials, Shangluo University, Shangluo 726000, China.

*E-mail: slchunshengzhou@126.com

[‡]Key Laboratory of Synthetic and Natural Functional Molecule of the Ministry of Education, College of Chemistry and Materials Science, Northwest University, Xi'an 710127, China.

*E-mail: northwindy@126.com

Received July 3, 2020, Accepted October 11, 2020, Published online November 3, 2020

Keywords: Lead(II) compound, Acylhydrazone, Luminescence, Antifungal activity

The syntheses of metal–organic complexes have been widely explored due to their fascinating architectures and potential application as functional materials in gas storage, catalysis, magnetism, photoluminescence, and biological application.^{1–3} From the view of coordinated metal center, most metal–organic complexes are focused on *s*-, *d*-, and even *f*-block metals, while relatively little attention has been paid to the *p*-block Pb(II). In fact, the special electronic configuration ([Xe]4f¹⁴5d¹⁰6s²) of Pb(II), often gifts Pb(II) complexes unique performance in coordination chemistry, photochemistry, and biochemistry.^{4,5} To construct stable Pb(II) complexes, aromatic multidentate ligands with both soft and hard donor atoms might be a good choice.^{6,7} Aromatic acylhydrazones are well-known polydentate ligands,⁸ which bear both nitrogen and oxygen coordination sites, possessing strong capability to bind metal centers. Meanwhile, the –CO–NH–N=CH– group featuring hydrogen-bond donors or acceptors is apt to form stable supramolecular architectures.⁹ It is also worth noting that the acylhydrazone complexes with the special azomethine group often possess excellent biological and pharmacological activities, such as antibacterial,¹⁰ anticancer,¹¹ and antitumor.¹²

Recently, our laboratory group has focused on the construction, crystallographic characterization, and antibacterial activity of metal-hydrazone complexes under ambient conditions.^{13,14} Because of the strong chelating capability of N/O donors in acylhydrazone, these complexes are prone to form 0D mononuclear structures or discrete dimer.¹⁵ And rare metal–organic polymers have been reported, especially the Pb(II)-based ones owing to the elusive and variable coordination geometries and coordination numbers of 2 ~ 10 for lead(II) ions.¹⁶ Herein, a flexible multidentate ligand, *N*-(2-propionic acid)-2-(4-hydroxybenzoyl) hydrazone (**H₃L**),

was designed and synthesized to construct a bifunctional lead(II)-based coordination polymer [Pb(HL)]_n (**1**), which has been fully characterized by elemental analysis, IR spectroscopy, single-crystal X-ray diffraction and thermogravimetric analysis. The antifungal activity investigation reveals that **1** gives stronger antifungal ability than that of the ligand **H₃L** and Pb(II) because of the effective synergy between the metal and ligand. In addition, the strong blue fluorescence property and the non-isothermal thermokinetic analyses of the thermodecomposition of **1** were also investigated in detail.

Structural analysis reveals that **1** crystallizes in the monoclinic space group *P2₁/c*. The asymmetric unit contains one crystallographically independent Pb(II) ion and one partly deprotonated **HL**²⁻ ligand. As depicted in Figure 1, Pb1 ion is five-coordinated by one nitrogen atom (N2) and two oxygen atoms (O₂ and O₃) from one **HL**²⁻ ligand and two carboxylate oxygen atoms (O3A and O4A; symmetry code: A, *x*, –*y* + 3/2, *z* – 1/2) from another **HL**²⁻ ligand, resulting in a distorted trigonal bipyramid geometry (Figure 2(a)). According to the special holo-/hemisphere effects of Pb(II) described by Shimoni *et al.*,¹⁶ the coordination sphere of Pb(II) in **1** is classified to be typically hemidirected configuration, because the Pb–L (L = ligand) bonds are directed only to a part of the coordination sphere, leaving a gap in the distribution of bonds to the ligand. The Pb–O bond distances vary from 0.2333 (8) to 0.2512 (8) nm with a mean of 0.2429 (8) nm, while the average Pb–N bond distance is slightly shorter, 0.2395 (9) nm (Table S2). All of the bond lengths and angles in **1** are within normal ranges and comparable to those reported Pb(II)-acylhydrazone compounds.¹⁷

In **1**, the **HL**²⁻ ligands adopt a chelating-bridging μ_2 - η^2 : η^1 coordination mode (Figure 2(b)), and bridge adjacent

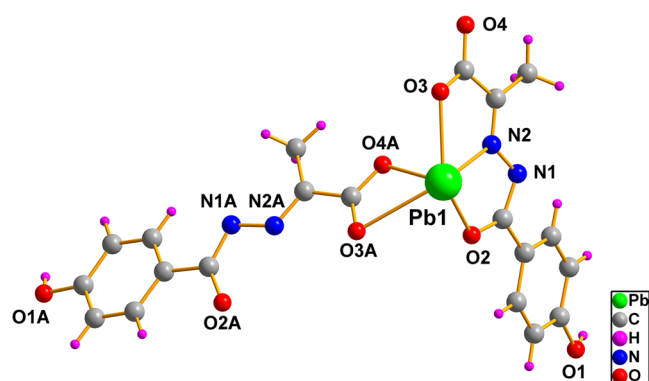


Figure 1. Coordination environment of Pb(II) in **1**. Symmetry code: A, x , $-y + 3/2$, $z - 1/2$.

Pb(II) centers to 1D infinite zigzag chains with the shortest intra-chain Pb...Pb separation of 0.5291 (3) nm (Figure 3). As shown in Figure 4, the hydroxyl oxygen atom O1 and the carboxylate oxygen atom O4 of the ligand participate in the formation of strong O—H...O H-bonds as donor and acceptor, respectively (Table S3), which ultimately connect the neighboring chains to yield a 3D supramolecular structure.

To study the thermal stability of **1**, the thermogravimetric analysis (TGA) was carried out under N₂ atmosphere with a heating rate of 10 °C min⁻¹ from 30 to 600 °C. As shown in Figure S1, TG curve indicates that **1** remains stable up to 260 °C, which could be attributed to the strong intermolecular O—H...O H-bonds occurring in the framework.¹⁸ Then the complex undergoes fast weight loss, which is due to the thermal decomposition of the organic ligands, yielding an unidentified product (the decomposition process does not stop before 600 °C).

Kissinger's method and OzawaDoyle's method are performed using differential scanning calorimetry (DSC) to investigate the thermoanalysis kinetic parameters such as the apparent activation energy (E) and the pre-exponential factor (A) of the thermodecomposition of **1**,^{19,20} which are universally applied in this field. The Kissinger and Ozawa-Doyle equations are as following, respectively:

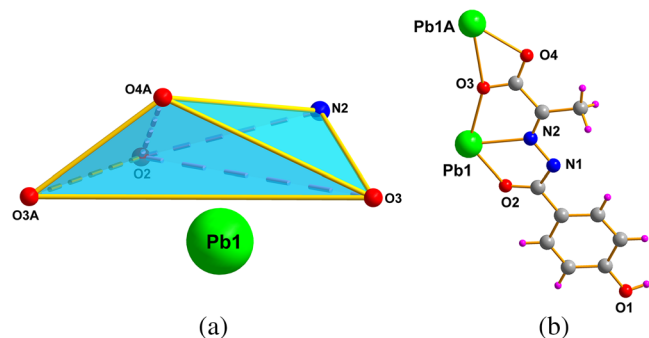


Figure 2. (a) Coordination polyhedron geometry of Pb(II) in **1**. Symmetry code: A, x , $-y + 3/2$, $z - 1/2$. (b) Coordination environment of the ligand in **1**.

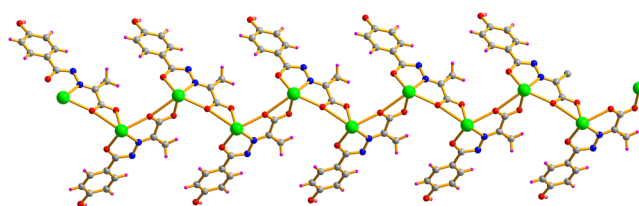


Figure 3. 1D infinite chain structure in **1**.

$$\frac{E\beta}{RT_p^2} = A \exp\left(-\frac{E}{RT_p}\right) \quad (1)$$

$$\lg\beta + \frac{0.4567E}{RT_p} = C \quad (2)$$

where T_p is the peak temperature (°C), R is the gas constant (J·mol⁻¹·°C⁻¹), β is the linear heating rate (°C·min⁻¹), A is the pre-exponential factor (s⁻¹), E is the apparent activation energy (kJ·mol⁻¹) and C is constant. Herein, the non-isothermal kinetics analysis is discussed based on the peak temperatures measured at four different heating rates of 2, 5, 8, 10 °C·min⁻¹ (Figure S2). In Table 1, obviously, the exothermic peak, T_p , shifts to higher temperatures with the heating rate increasing and the linear correlation coefficients are very close to 1, indicating that the results are credible. The values of E_a (the average of E_k and E_o) are 193.36 kJ·mol⁻¹. The Arrhenius Equations are expressed as follows: $\ln k = 14.547 - 193.36 \times 10^3/RT$ for **1**, which can be used to figure out the rate constants of the initial thermal decomposition process of **1**.

The fluorescence spectra of **1** and free ligand (**H₃L**) were examined in the solid state at room temperature. As shown in Figure 5, an intense emission of the free **H₃L** ligand was observed in the wavelength range of 430–470 nm ($\lambda_{\max} = 447$ nm upon excitation at 380 nm). Complex

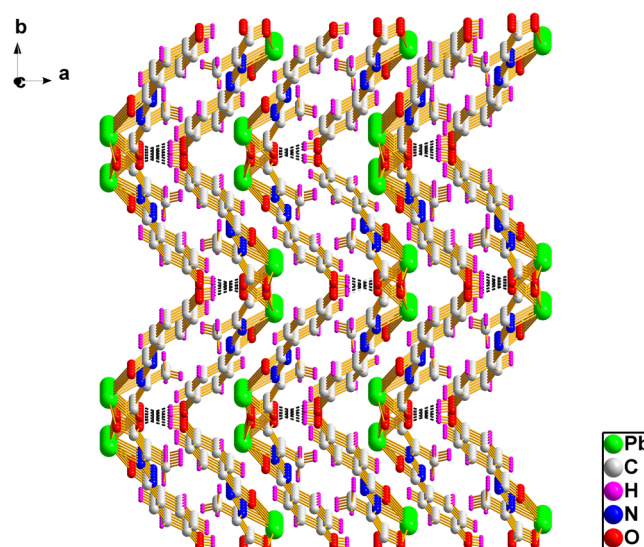


Figure 4. 3D supramolecular architecture of **1** assembled via inter-chain O—H...O hydrogen bonds (black dashed lines).

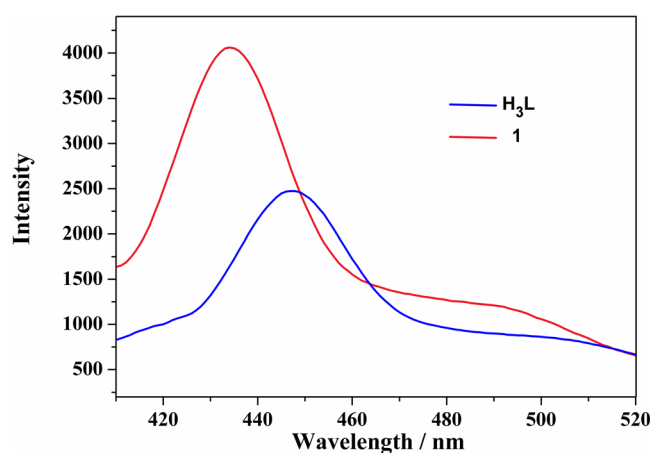


Figure 5. Solid-state emission spectra of H_3L (blue line) and complex **1** (red line) at room temperature.

1 exhibits photoluminescence with an emission maximum at 434.6 nm upon excitation at 380 nm. It is not difficult to find that the emission of **1** has similar profile observed in the free H_3L ligand but presents slightly blue-shifted emission band, suggesting that the emission band of **1** originates from the π - π^* or π - n transitions within the ligand and the shift may be due to the ligand-to-metal charge transfer (LMCT).^{7,18} The emission quantum yields (Φ_F) of **1** and H_3L were determined to be 23.4% and 2.6%, respectively. Compared to the free H_3L ligand, the fluorescence intensity and Φ_F of **1** are significantly increased, which may be because the coordination limits the twist of acylhydrazone group and increases the whole rigidity of the ligand.

Given the good biological and pharmacological activities of acylhydrazones,^{10–12} the antibacterial abilities of the complex **1** and H_3L against the fusarium fungi were evaluated. Before tests, the phase purity of the powder microcrystalline samples of **1** is confirmed by PXRD (Figure S5), and the molar conductance value of complex **1** is determined to be $16.5 \text{ S cm}^2 \text{ mol}^{-1}$ in DMF, suggesting that **1** is nonelectrolyte. According to the antifungal screening data from Table 2 and Table S4, the toxicity of compound **1** is 6.15 times higher than that of H_3L , as well as 2.42 times higher than that of PbCl_2 , which reveals that the complex **1** shows remarkable inhibitory effect on the fusarium fungi. Notably, **1** shows much better inhibitory activity against the tested fungi than those previously reported acylhydrazone based complex in our group,¹³ which may be ascribed to the superior activity of the hemidirected Pb(II) cation in **1**.^{21,22} Moreover, the effect of

the counter ion of the lead salts on the antifungal activity were also discussed (Table 2). The results of bioassay indicate that the fungicidal activities of the three inorganic lead salts against the fusarium fungi do not show apparent diversity, which suggests that the bioactivity of **1** depends only on the synergistic effects of the HL^{2-} ligand and metal ion and not on the counter anions. The possible mechanism for the synergistic effect on antifungal activity of **1** can be concluded: the hemidirected Pb(II) cation as the unsaturated active center is conducive to interact with the active groups (N or O sites) of the coat protein discs of the fusarium fungi by coordination activation, while the acylhydrazone ligand containing rich H-bond donor site (hydroxyl group) and acceptor site (amide group) can further inhibit fusarium fungi activities by direct binding the coat protein discs through hydrogen bonds, ultimately leading to the disassembly of the coat protein discs into monomers and an almost complete loss of pathogenicity.²³ Since the synthesized complex could be taken for the molecular-level mixtures of HL^{2-} and inorganic lead salts, the synergy ratio (SR) was employed to evaluate the extent of the interactions between HL^{2-} and Pb(II) that was tested against the fusarium fungi according to the Wadley approach.²⁴ Apparently, the obtained SR value of 3.48 (> 1.5) reveals that the interaction level was synergistic.

In summary, a bifunctional Pb(II)-based coordination polymer $[\text{Pb}(\text{HL})]_n$ (**1**) was constructed by the multidentate acylhydrazone ligand, *N*-(2-propionic acid)-2-(4-hydroxybenzoyl) hydrazone (H_3L) and fully characterized. Structural analysis indicates that **1** features a 3D supramolecular framework generated by strong intermolecular O–H...O H-bonds bridging 1D infinite zigzag chains. The polymer **1** exhibits good thermostability ($> 260^\circ\text{C}$) and strong blue fluorescence. The non-isothermal kinetic parameters of the exothermic thermodecomposition process for **1** were investigated based on the Kissinger's and Ozawa-Doyle's methods, and the value of the apparent activation energy was calculated to be $193.36 \text{ kJ mol}^{-1}$. Furthermore, **1** shows noticeable inhibitory effect on the fusarium fungi because of the synergistic action of the hemidirected Pb(II) cation and the acylhydrazone ligand, and its toxicity is 6.15 times higher than that of H_3L , as well as 2.42 times higher than that of PbCl_2 .

Experimental

Preparation of H_3L . Five drops of acetic acid were added to a mixture of 4-hydroxybenzoic acid hydrazide (1.52 g, 10 mmol) and 2 mL pyruvic acid (2.45 g, 27.88 mmol) in a

Table 1. Peak temperatures and the thermoanalysis kinetic parameters of the exothermic decomposition reaction of **1**.

β ($^\circ\text{C}\cdot\text{min}^{-1}$)	T_p ($^\circ\text{C}$)	$\lg(A_k/\text{s}^{-1})$	R_k	R_o	E_k ($\text{kJ}\cdot\text{mol}^{-1}$)	E_o ($\text{kJ}\cdot\text{mol}^{-1}$)	E_a ($\text{kJ}\cdot\text{mol}^{-1}$)
2	315.2	14.547	0.9911	0.9919	193.36	193.35	193.36
5	325.6						
8	334.3						
10	338.8						

Table 2. Antifungal activities of **1**, **H₃L** and different lead salts against fusarium.

Sample	Drug concentration-effect curves	R ²	EC ₅₀ (mg L ⁻¹)	SR
1	$y = 4.7055x + 2.8972$	0.9911	2.80	3.48
H₃L	$y = 4.9715x - 0.9227$	0.9970	17.22	
PbCl ₂	$y = 5.5629x + 0.374$	0.9982	6.78	
Pb(NO ₃) ₂	$y = 5.6958x - 0.0274$	0.9972	7.63	
Pb(Ac) ₂	$y = 5.5463x + 0.071$	0.9943	7.74	

dry EtOH solution (30 mL). The mixture was heated at 75°C over 6 h and a white precipitate was isolated by filtration, recrystallized from alcohol and washed by ether, dried under vacuum. Yield: 71%. Anal. Calcd. (%) for C₁₀H₁₀N₂O₄: C, 54.05; H, 4.54; N, 12.61. Found: C, 54.18; H, 4.26; N, 12.91. ¹H NMR (400 MHz, DMSO-*d*₆), δ (ppm): 12.88 (brs, 1H), 11.29 (s, 1H), 7.80 (d, *J* = 8.7 Hz, 2H), 6.85 (d, *J* = 8.7 Hz, 2H), 3.81 (s, 1H), 2.14 (s, 3H). IR(KBr, cm⁻¹): 3437(m), 3254(m), 3193(w), 2994(w), 2804(w), 2672(w), 1686(s), 1655(s), 1620(s), 1598(s), 1534(s), 1505(s), 1491(m), 1384(m), 1348(s), 1283(s), 1256(m), 1224(s), 1125(m), 998(m), 854(m), 821(s), 754(m), 589(m).

Preparation of [Pb(HL)]_n. A mixture of 5 mL of CH₃OH/DMF (v:v = 1:1) was layered carefully on an aqueous solution of Pb(NO₃)₂ (33.1 mg, 0.1 mmol) (5 mL). Then, a 5 mL of **H₃L** (22.2 mg, 0.1 mmol) methanol solution was further layered above on the mixed solutions. The container was sealed up and kept in dark place for a few days. Colorless block crystals were ultimately obtained with a yield of 42% (based on Pb²⁺) (Figure S6). Anal. Calcd. (%) for **1** (C₁₀H₈N₂O₄Pb): C, 28.10; H, 1.89; N, 6.55. Found: C, 28.56; H, 2.65; N, 6.63%. IR(KBr, cm⁻¹): 3212(m), 2813(w), 2708(w), 2686(m), 1694(s), 1634(s), 1599(s), 1501(s), 1482(m), 1386(m), 1348(s), 1294(s), 1240(m), 1209(s), 1010(m), 914(m), 841(w), 787(w), 760(m), 706(w), 680(w), 654(w), 595(m), 533(w). The white powder microcrystalline samples of **1** were obtained with a yield of 78% by direct mixing 20 mL of **H₃L** methanol solution (0.05 M) and 20 mL of Pb(NO₃)₂ aqueous solution (0.05 M) over 1 h.

Acknowledgments. This work was financially supported by the National Natural Science Foundation of China (Nos. 21703135 and 21803042), the Nature Science Basic Research Program of Shaanxi (Nos. 2019JQ-249 and 2019JQ-067), the Natural Science Foundation of the Department of Education of Shaanxi Province (No. 17JS034), the Outstanding Young Talents Fund of University in Shaanxi Province (18SKY001), the 64th China Postdoctoral Science Foundation Funded Project (2018M643706), the Innovative and Entrepreneurial Training Program for Shaanxi Province College Students (No. S201911396001) and the Natural Science Foundation of Shangluo University (No. 19SKY003).

Supporting Information. Additional supporting information may be found online in the Supporting Information section at the end of the article.

References

- Y. B. He, W. Zhou, G. D. Qian, B. L. Chen, *Chem. Soc. Rev.* **2014**, *43*, 5657.
- J. Liu, L. Chen, H. Cui, J. Zhang, L. Zhang, C. Y. Su, *Chem. Soc. Rev.* **2014**, *43*, 6011.
- Z. Hu, B. J. Deibert, J. Li, *Chem. Soc. Rev.* **2014**, *43*, 5815.
- M. H. Jack, M. Saeed, A. S. Ali, *Inorg. Chem.* **2004**, *43*, 1810.
- J. Li, Y. Lu, *J. Am. Chem. Soc.* **2000**, *122*, 10466.
- S. R. Fan, L. G. Zhu, *Inorg. Chem.* **2006**, *45*, 7935.
- Z. Wang, Q. Wei, G. Xie, Q. Yang, S. P. Chen, S. L. Gao, *J. Coord. Chem.* **2012**, *65*, 286.
- M. Hong, H. D. Yin, J. C. Cui, *Solid State Sci.* **2011**, *13*, 501.
- P. Malakar, E. Prasad, *Chem. A Eur. J.* **2015**, *21*, 5093.
- C. Santini, M. Pellei, V. Gandin, M. Porchia, F. Tisato, C. Marzano, *Chem. Rev.* **2014**, *114*, 815.
- J. Deng, W. Chen, H. Deng, *J. Fluoresc.* **2016**, *26*, 1987.
- C. Congiu, V. Onnis, *Bioorg. Med. Chem.* **2013**, *21*, 6592.
- C. F. Qiao, L. Sun, S. Zhang, Q. Wei, C. S. Zhou, G. Xie, S. P. Chen, X. W. Yang, S. L. Gao, *Polyhedron* **2016**, *119*, 445.
- Y. Liu, Y. Di, Y. Di, C. Qiao, F. Chen, F. Yuan, K. Yue, C. Zhou, *J. Mol. Struct.* **2019**, *1184*, 532.
- M. Hong, H. Yin, S. Chen, D. Wang, *J. Organomet. Chem.* **2010**, *695*, 653.
- L. Shimon-Livny, J. P. Glusker, C. W. Bock, *Inorg. Chem.* **1998**, *37*, 1853.
- K. K. Du, *Chin. J. Struct. Chem.* **2012**, *31*, 1842.
- Z. Q. Xia, Q. Wei, Q. Yang, C. F. Qiao, S. P. Chen, G. Xie, G. C. Zhang, C. S. Zhou, S. L. Gao, *CrystEngComm* **2013**, *15*, 86.
- T. Ozawa, *Bull. Chem. Soc. Jpn.* **1965**, *38*, 1881.
- R. Z. Hu, S. L. Gao, F. Q. Zhao, Q. Z. Shi, T. L. Zhang, J. J. Zhang, *Thermal Analysis Kinetics*, Science Press, Beijing, **2007**.
- H. Xiao, A. Morsali, *Solid State Sci.* **2007**, *9*, 155.
- N. Noshiranzadeh, A. Ramazani, A. Morsali, A. D. Hunter, M. Zeller, *Inorg. Chem. Commun.* **2007**, *10*, 738.
- Z. Wang, D. Xie, X. Gan, S. Zeng, A. Zhang, L. Yin, B. Song, L. Jin, D. Hu, *Bioorg. Med. Chem. Lett.* **2017**, *27*, 4096.
- F. M. Wadley, *Experimental Statistics in Entomology*, Graduate School Press, Washington State University, Pullman, **1976**.